Journal of Natural Resource Conservation and Management
Vol. 4, No. 1, pp 15-29, 2023
doi: 10.51396/ANRCM.4.1.2023.15-29

Identification of hydrogeochemical processes affecting the hydrochemistry of groundwater: A review

Jashandeep Singh Sidhu and Sumita Chandel*

Department of Soil Science, Punjab Agricultural University, Ludhiana-141004, Punjab, India
**Corresponding author Email: Sumita-soasoil@pau.edu*

Received : March 04, 2023
Revised : April 11, 2023
Accepted : May 24, 2023
Published : June 30, 2023

ABSTRACT

Hydrogeochemical processes are the processes that bring seasonal and spatial fluctuations in groundwater chemistry. These include rock-water interactions, ion exchange, evaporation, and other natural processes that affect groundwater as it flows from one location to another or as it remains at one location. Numerous ionic ratios, scatter plots, and diagrams are available for the identification of these processes. Ion exchange is an important contributor to groundwater chemistry and is of two types: direct ion exchange and reverse ion exchange. Rock-water interaction is another significant mechanism because the mineral content and formation of rocks through which groundwater flows, will influence its chemical composition. There are two major natural weathering processes, involving carbonic acid and sulphuric acid as the weathering agents. The ratios of Ca: HCO_3 and Ca: SO_4 help to identify the type of carbonate mineral being dissolved by these two acids. Groundwater chemistry is also impacted by anthropogenic factors like mining activities and improper disposal of industrial and sewage waste that can increase the concentration of nitrate and several heavy metals in it. The concentration of ions present in groundwater can be used to categorize it into different hydrogeochemical facies using Piper and Chadha diagrams. Identification of these hydrogeochemical processes helps to figure out the primary source of contamination of groundwater. We have tried to compile the information in one document. These processes provide an idea about mineral composition and hence the hydrogeology of the area. However, no single approach can reliably identify a certain process, we require a combination of indicators for this, that can help to develop different hydrogeochemical models for the prediction of groundwater quality.

Keywords: Groundwater, hydrogeochemical processes, ionic ratios, rock-water interaction, anthropogenic activities

INTRODUCTION

Groundwater plays a major role in sustainable development all over the world, especially in arid and semi-arid regions. It is an essential resource for millions of people not only for drinking but also for irrigation. The groundwater quality is equally essential as the quantity because it acts as the primary determinant of its usefulness for drinking, residential, and industrial purposes (Kaur *et al.,* 2017). According to the previous estimates, groundwater provides 35 percent of the global home water supply, 40 per cent for irrigation, and 24 percent for industrial functions (GEF 2022). However, due to rapid population growth, intensive agriculture, mining, industrialization, climate change, and geogenic activities groundwater resources are under stress (Zia *et al.,* 2017; Kumar *et al.,* 2020). The chemical composition of groundwater is also heavily affected by its interaction with the minerals of the aquifer through which it travels. The mechanism that controls the chemical composition of the dissolved salts in groundwater has been discussed by many scientists. However, to understand the overall mechanism there is a need to identify and understand major hydrogeochemical processes occurring in groundwater affecting its hydrochemistry. The

hydrogeochemical mechanisms that change the chemical composition of groundwater are spatially and temporally variable. Due to a variety of processes such as soil/rock–water interactions, prolonged storage in the aquifer, and dissolution of mineral species, groundwater in any location has a distinct chemistry (Subramani *et al.,* 2010). The hydrogeochemical processes are defined as the operations that take place during the movement of groundwater from one place to another. The hydrogeochemical processes that are known to affect groundwater chemistry are rock-water interactions, precipitation, evaporation, ion exchange, and leaching. There are different ionic ratios, diagrams, and scatter plots for identifying the dominant process among them. These methods of identification are being modified from time to time and new ideas are also being introduced by various scientists throughout the world. Identification of these processes is necessary to recognize the primary source of contamination of groundwater and to design suitable management plans, that will decrease their adverse effects (Kumar *et al.,* 2009). An attempt has been made to review and discuss different hydrogeochemical processes that affect the hydrochemistry of groundwater by studying the Gibbs diagram, scatter plots, ionic ratios, weathering pathways, Piper diagram and Chadha diagram. This will help to elucidate the major mechanism controlling the hydrogeochemistry of groundwater.

A. GIBBS DIAGRAM

Gibbs (1970) studied major natural mechanisms that control the world's water chemistry. Ca^{2+} and Na^{+} are the primary cations for fresh and high-saline water bodies respectively, that characterise the end-members of earth's surface waters. This plot has the weight ratio $Na^{+}/ (Na^{+} + Ca^{2+})$ on the x-axis and the fluctuation in total salinity on the y-axis and studies the composition of the world's surface waters. The proposed diagram (Fig. 1a) represents the three significant processes (Rock-water interactions, precipitation, and evaporation) controlling the water ion composition. The proposed diagram is based on two plots, both having TDS on the y-axis, while $Na^{+}/ (Na^{+} + Ca^{2+})$ on the x-axis for one plot and $Cl^{-} / (Cl^{-} + HCO_3^{-})$ for the other plot. It is widely used by scientists for the identification of the dominant process among these three natural processes. Fig. 1b presents the Gibbs diagram of Coimbatore, Tamil Nadu which identifies the rock-water interaction as the major process, while a few samples also lie in the evaporation zone. This indicates that evaporation is also a contributing factor in arid and semi-arid climates (Kumar & James, 2016)

B. EVAPORATION

Evaporation is a common phenomenon in semi-arid and arid environments. The shallow water level and large number of wells can assist evaporation in altering the groundwater chemistry. The contribution of evaporation in groundwater chemistry can be identified using the Gibbs diagram, but sometimes it does not accurately predict its dominance. As shown in Fig.1b, the effect of evaporation does exist in the Coimbatore region but it is not enough to highly affect the groundwater chemistry in other words, its dominance is not

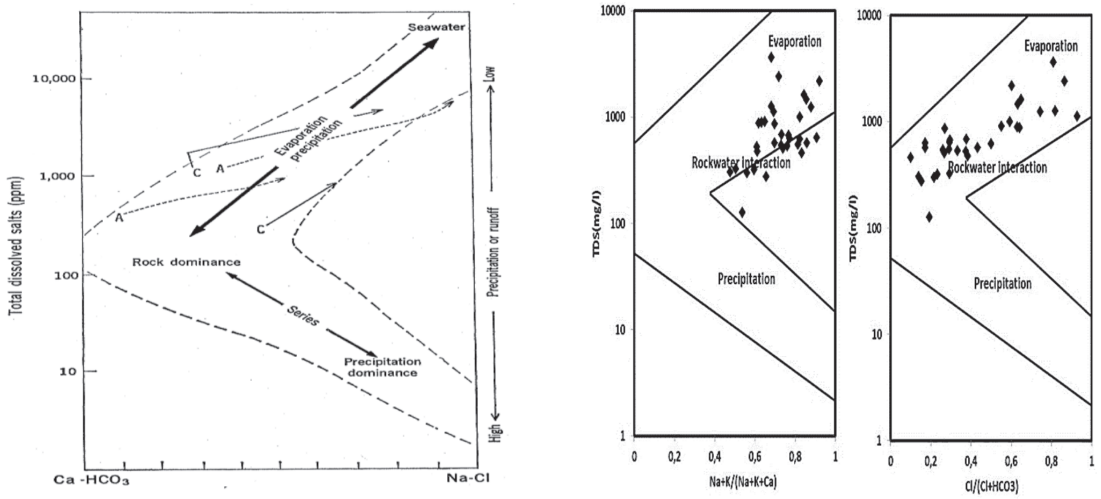

Fig. 1. a) Diagrammatic representation of processes affecting water chemistry (*Source:* Gibbs, 1970), b) Gibbs plot reflecting the geochemical processes in Coimbatore (*Source:* Kumar & James, 2016)

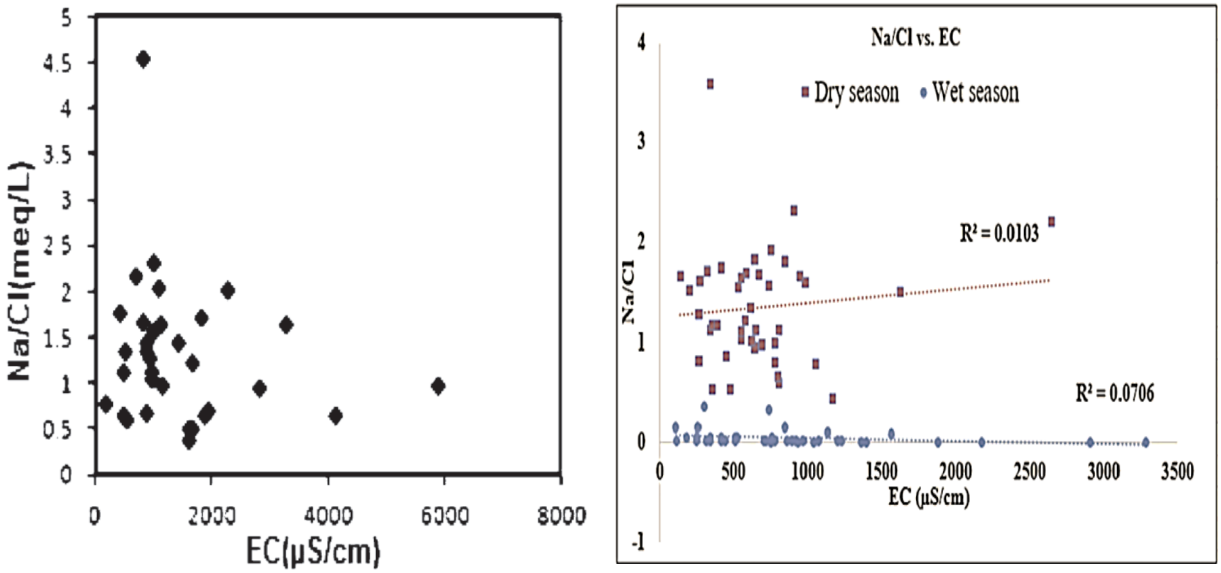

Fig. 2. a) Na^+/ Cl^- vs EC plot of Coimbatore, Tamil Nadu (*Source:* Kumar & James, 2016), b) Na^+/ Cl^- vs EC plots of wet and dry seasons of south-west Nigeria (*Source:* Yusuf *et al*., 2021)

predictable. For this, the Na^+/Cl^- vs. electrical conductivity plot can be used effectively. The effect of this process is such that TDS concentrations rise as a result of evaporation, while the Na/Cl ratio remains unchanged with an assumption that mineral species are not precipitated (Jankowski & Acworth 1997). This indicates that as EC increases, the ratio of Na^+ to Cl^- must remain constant. Fig. 2a depicts that the Na^+/Cl^- vs EC plot shows a negative correlation in Coimbatore, Tamil Nadu. This suggests that evaporation isn't the only factor in determining groundwater chemistry but ion exchange or silicate weathering are two further possibilities for changing the ratio (Kumar & James 2016). Na^+/Cl^- vs EC graph (Fig. 2b) of the southwest region of Nigeria, clearly shows that Na+/ Cl- is constant during the wet season indicating evaporation as the dominant process, while during the dry season, there is a slight variation in Na^+/Cl^- ratio with EC. Evaporation is dominant during the wet season of the region because of the mixture of nearby highly evaporated surface brackish water with the shallow groundwater (Yusuf *et al.,* 2021).

C. ION EXCHANGE

In semi-arid environments, ion exchange is an important activity that contributes to the chemistry of water. In the normal ion exchange process, the Ca^{2+} present in groundwater will replace the Na^+ adsorbed on clay as shown in equation 1 (Kumar & James, 2016). Desirable conditions for the ionic exchange process to occur are a replenished source of groundwater with enhanced Ca^{2+} levels along with minerals having significant cation exchange capacity with Na^+ on the exchange sites (Cloutier *et al.,* 2010). The reverse ion exchange process is exactly the opposite where Na^+ ions present in groundwater replace the Ca^{2+} ions and get adsorbed on clay particles as shown in equation 2. Reverse ion exchange can cause soil dispersion and clogging of pores due to Na^+ adsorption.

- $Ca^{2+} + Na^+$–clay ——— Ca^{2+}–clay + Na^+ …. (Ion exchange process) (eq. 1)
- $Na^+ + Ca^{2+}$–clay ——— Na^+–clay + Ca^{2+} …. (Reverse ion exchange process) (eq. 2)

Ion exchange is identified by different ionic ratios as:

1. Chloro-alkaline index
2. $(Ca^{2+} + Mg^{2+} - HCO_3^- - SO_4^{2-})$ v/s $(Na^+ - Cl^-)$ plot
3. $(Ca^{2+} + Mg^{2+})$ v/s $(SO_4^{2-} + HCO_3^-)$ plot
4. Na^+/Cl^- vs EC
5. Ca^{2+} v/s Na^+

1. Chloro-alkaline index

Chloro-alkaline (CAI) index helps to realize the ion exchange relationship between groundwater and the surrounding rocks (Schoeller 1967). It is calculated by two equations called Chloro-alkaline

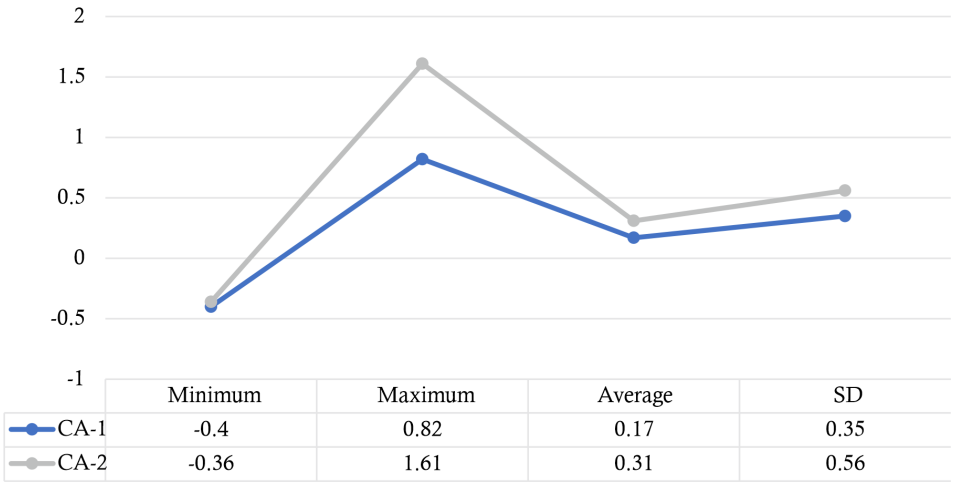

	Minimum	Maximum	Average	SD
CA-1	-0.4	0.82	0.17	0.35
CA-2	-0.36	1.61	0.31	0.56

Fig. 3. Chloro-alkaline indices of Rajpur region, Andhra Pradesh (*Source:* Nagaraju *et al.*, 2016)

index 1 (CAI-1) and Chloro-alkaline index 2 (CAI-2) as mentioned in eq. 3 and eq. 4 respectively

- $CAI\text{-}1 = (Cl^- - Na^+ + K^+)/Cl^-$ (eq. 3)
- $CAI\text{-}2 = (Cl^- - Na^+ + K^+)/ (SO_4^{2-} + HCO_3^- + NO_3^-)$ (eq. 4)

If both CAI-1 and CAI-2 are positive then it reflects that ion exchange occured between Na^+ or K^+ present in groundwater with that of Mg^{2+} or Ca^{2+} from host rocks i.e., reverse-ion exchange process is significant, whereas the negative value indicates a complete opposite process showing the dominance of direct ion exchange process (Adimalla 2020). The average chloro-alkaline index of the Rajpur area of Andhra Pradesh is positive, indicating the reverse ion exchange process is dominant in the region (Fig. 3). However specifically it can be said that since CAI-1 ranged between -0.40 and 0.82, whereas CAI-2 ranged between -0.36 to 1.61 (Fig. 3). Hence, few samples in the research area fall into negative zones, while others lie in positive zones (Nagaraju *et al.,* 2016).

2. $(Ca^{2+} + Mg^{2+} - HCO_3^- - SO_4^{2-})$ v/s $(Na^+ - Cl^-)$ plot

In this scatter diagram, $(Na^+ - Cl^-)$ is plotted on the x-axis, while $(Ca^{2+}+Mg^{2+}-HCO_3^--SO_4^{2-})$ is plotted on the y-axis. The Cl^- and SO_4^{2-} concentrations, represent the quantity of dissolved halite and gypsum, respectively. The net amount of dissolved calcite and dolomite is recorded by HCO_3^-. Thus, $(Ca^{2+}+ Mg^{2+}- SO_4^{2-}- HCO_3^-)$ reflects the amount of Ca^{2+} and Mg^{2+} acquired or lost relative to that given by gypsum, calcite, and dolomite dissolution, whereas Na^+- Cl^- determines the amount of Na^+ gained or lost compared to that provided by the dissolution of halite. If the slope of the relation between these two factors is exactly -1.0, then this indicates the existence of a reverse ion exchange process, provided that cation exchange is a substantial composition-controlling activity (Fisher & Mullican 1997). Fig. 4a represents the $(Na^+ - Cl^-)$ v/s $(Ca^{2+} + Mg^{2+} - HCO_3^- - SO_4^{2-})$ plot of the Lar area of Iran, There is a trend towards the formation of a clear -1 slope line, showing the influence of reverse ion exchange in the region (Rezaei *et al.,* 2017).

3. $(Ca^{2+} + Mg^{2+})$ v/s $(SO_4^{2-} + HCO_3^-)$ plot

The scatter diagram of $(Ca^{2+} + Mg^{2+})$ v/s $(SO_4^{2-} + HCO_3^-)$ helps in the identification of the ion exchange process. Here $(Ca^{2+} + Mg^{2+})$ is plotted on the y-axis and $(SO_4^{2-} + HCO_3^-)$ on the x-axis. If the samples lie close to a 1:1 slope then this will indicate the dissolution of calcite ($CaCO_3$), gypsum ($CaSO_4$), and dolomite [$CaMg(CO_3)_2$]. The chemical formulation of these minerals is such that in the end these will give an equal number of ions on dissolution (Datta & Tyagi 1996). However, if the groundwater samples are plotted above the 1:1 line i.e., towards the y-axis indicating higher $(Ca^{2+}+ Mg^{2+})$ in groundwater then it depicts the existence of a reverse ion exchange process (Rezaei *et al.,* 2017). On the contrary, if the plots lie below the 1:1 line then it shows the presence of a direct ion exchange process. In the $(Ca^{2+} + Mg^{2+})$ v/s $(SO_4^{2-} + HCO_3^-)$ scatter diagram of the Lar area of Iran (Fig. 4b), the majority of the plots lie above the 1:1 line depicting the reverse-ion exchange process in a given region (Rezaei *et al.,* 2017).

4. Na^+/Cl^- vs EC plot

Na^+/Cl^- v/s EC plot predicts the existence of an ion exchange process. Since no single scatter diagram can precisely indicate the presence of a particular process, we need several identifiers to predict a specific process. In this plot, Na^+/Cl^- is plotted on the y-axis and EC on the x-axis. During the direct ion exchange mechanism, the concentration of Na^+ ions increases in groundwater while there is no effect of this process on Cl^- concentration. However, the increase in Na^+ concentration may be due to other factors like silicate weathering (Kumar & James 2016), but there are other indicators to determine the dominance of silicate weathering. On the contrary, the reverse ion exchange process will decrease the Na^+/Cl^- ratio due to a decrease in Na^+ concentration. But if the Na^+/Cl^- ratio comes out to be exactly one or close to one then this indicates halite (NaCl) dissolution, because it gives equal concentration of Na^+ and Cl . In arid and semiarid regions having annual precipitation of less than 600 mm, the availability of free halite for dissolution in the soil zone could increase (Elango & Kannan 2007). On the scatter diagram, the plots lying above the aquiline indicate the ion exchange being prominent and vice-versa for the reverse ion exchange mechanism. In the Na^+/Cl^- vs EC plot of Lar, Iran, all the groundwater samples are plotted below the 1:1 line (Fig. 4c) indicating the dominance of the reverse ion exchange process (Rezaei *et al.,* 2017).

5. Na^+ v/s Ca^{2+} plot

If the points in this scatter plot are above the 1:1 line, the higher level of sodium ions suggests direct ion exchange, whereas those below the equiline, indicate reverse-ion exchange. Fig. 4d presents a plot of Na^+ v/s Ca^{2+} of the north region of the Densu

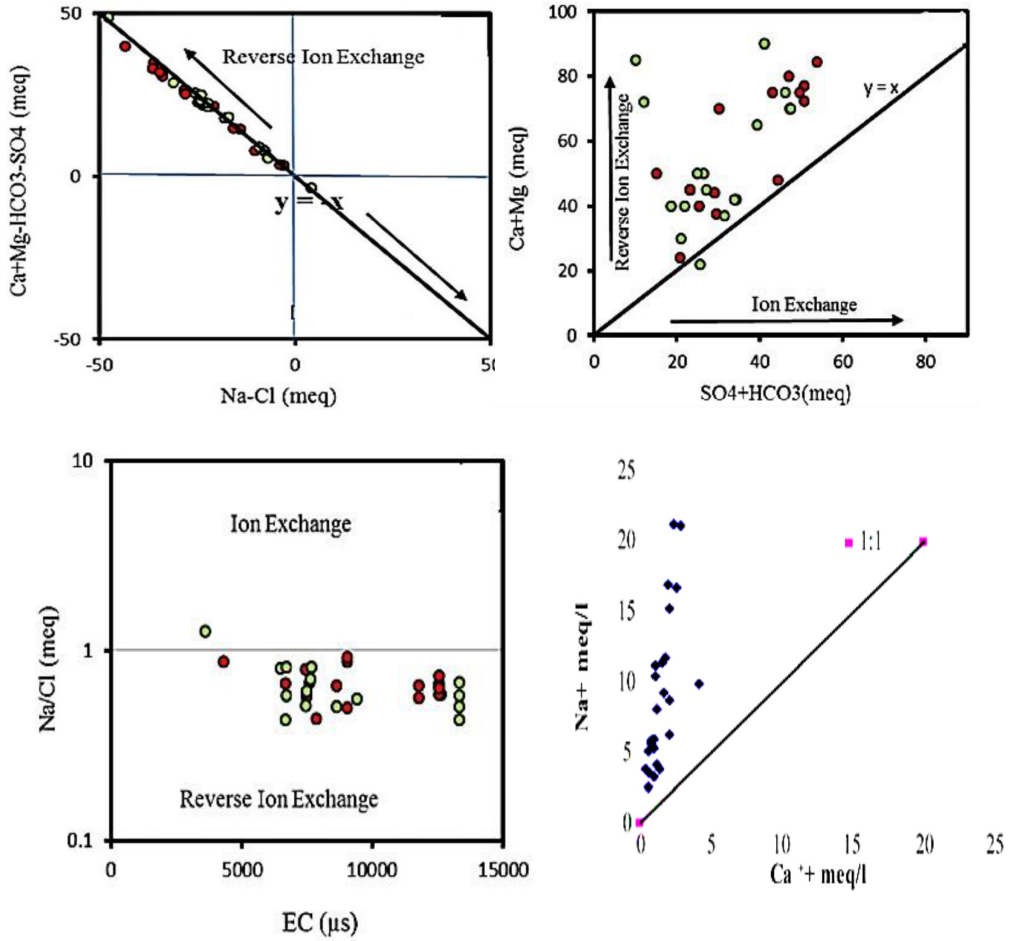

Fig. 4. Scatter plot diagrams showing ion and reverse ion exchange for various locations. a) (Ca^{2+} + Mg^{2+} - HCO_3^- - SO_4^{2-}) v/s (Na^+ - Cl^-) plot of Lar, Iran (*Source:* Rezaei *et al.*, 2017), b) (Ca^{2+} + Mg^{2+}) v/s (SO_4^{2-} + HCO_3^-) plot of Lar, Iran (*Source:* Rezaei *et al.*, 2017), c) Na^+/Cl^- vs EC plot of Lar, Iran (*Source:* Rezaei *et al.*, 2017), and d) Na^+ v/s Ca^{2+} plot of the Densu river basin of Ghana (*Source:* Gibrilla *et al.*, 2010)

River basin, Ghana. The scatter diagram with the data plotting above the aquiline line indicates an excess of Na^+ over Ca^{2+}, which might be attributable to the well's closeness to the clay strata. This indicates ion exchange mechanism is the reason behind the greater concentration of Na^+ ions in groundwater (Gibrilla *et al.,* 2010).

D. ROCK-WATER INTERACTIONS

The chemistry of groundwater is mostly determined by the mineral content and the formation through which it flows because of rock–water interactions. Evaporation and precipitation also alter the chemical composition of groundwater, but solid phases (inorganic and organic materials) are the principal suppliers and sinks of solubilized elements in groundwater, so rock–water interaction is the most important mechanism. A range of chemical interactions with solid phases occurs during groundwater migration throughout its route from recharge to discharge sites. Depending on the chemical makeup of the original water, geological formations, and residence period, these chemical reactions will vary geographically and temporally. The concentrations of key ions in groundwater that arise can be utilized to determine the degree of rock–water contact and chemical processes (Elango & Kannan 2007). Igneous, metamorphic, and sedimentary rocks are the three main kinds of Rocks. Chemical weathering resistance determines whether minerals in these rocks dissolve fully or partially in water. Weathering, dissolution, as well as oxidation, and reduction, occur during the contact between rock and water (Table 1). These chemical processes can bring rise and fall of ion concentration in groundwater; movement of dissolved components and variation in the pH of groundwater (Elango & Kannan 2007). Groundwater's chemical composition is thought to be the fingerprints of rock–water interaction and different chemical processes.

Calcite, dolomite, and gypsum weathering can provide Ca^{2+}, Mg^{2+}, CO_3^{2-} and SO_4^{2-} ions into the groundwater. The origin of HCO_3^- ions is from the soil and atmospheric CO_2 during the weathering of all the minerals with carbonic acid, particularly from carbonate minerals (Meybeck 1987). The major contributor of Na^+ ions in groundwater is halite weathering due to its low resistance to weathering (Table 1). However, silicate weathering particularly Albite (Na^+ plagioclase), Amphibole, and Pyroxene minerals also add Na^+ as well as HCO_3^- in groundwater as shown below in the reaction (5):

$$2NaAlSi_3O_8 + 2H_2CO_3 + 9H_2O \rightarrow \underset{\text{(albite)}}{} \quad Al_2Si_2O_5(OH)_4 + 2Na^+ + 4H_4SiO_4 + 2HCO_3^- \quad \text{(eq. 5)}$$
(Kaolinite)

Halite acts as the source of Cl^- ions in groundwater. The weathering of K-Feldspar and the use of synthetic fertilizers are possible sources of potassium in groundwater. However, low potassium levels in groundwater are owing to feldspar's higher resistance to weathering and fixing in the form of clay minerals, which results in nutrient loss (Kolahchi & Jalali, 2007). A major source of fluoride

Table 1. Different chemical mechanisms during rock–water interactions along with common minerals and their composition

Minerals and their chemical composition	Relative resistance to weathering	Mechanism of chemical weathering
Halite:(NaCl)	Too less	Dissolution
Gypsum:($CaSO_4.2H_2O$)	Too less	Dissolution
Pyrite:(FeS_2)	Less	Oxidation and Dissolution
Calcite:($CaCO_3$)	Less	Dissolution
Dolomite: [$CaMg(CO_3)_2$]	Less	Dissolution
Olivine: [(Fe, Mg) SiO_4]	Moderately less	Hydrolysis, oxidation
Pyroxene:(Ca, Na, Mg, Al, Fe silicates)	Medium	Hydrolysis, oxidation,
Plagioclase:($NaAlSi_3O_8$; $CaAl_2Si_2O_8$)	Medium	Hydrolysis
Hornblende (Amphibole):(Ca, Mg, Na, Al, Fe silicates)	Medium	Hydrolysis, oxidation
Biotite:(Mg, Fe, K, Al silicate)	Medium	Hydrolysis, oxidation
K-feldspar:($KAlSi_3O_8$)	Moderately high	Hydrolysis
Muscovite:(Al, K silicate)	High	Hydrolysis
Quartz:(SiO_2)	Quite high	Slow dissolution
Clays:(Al silicates)	Quite high	Hydrolysis

Source: Elango & Kannan (2007)

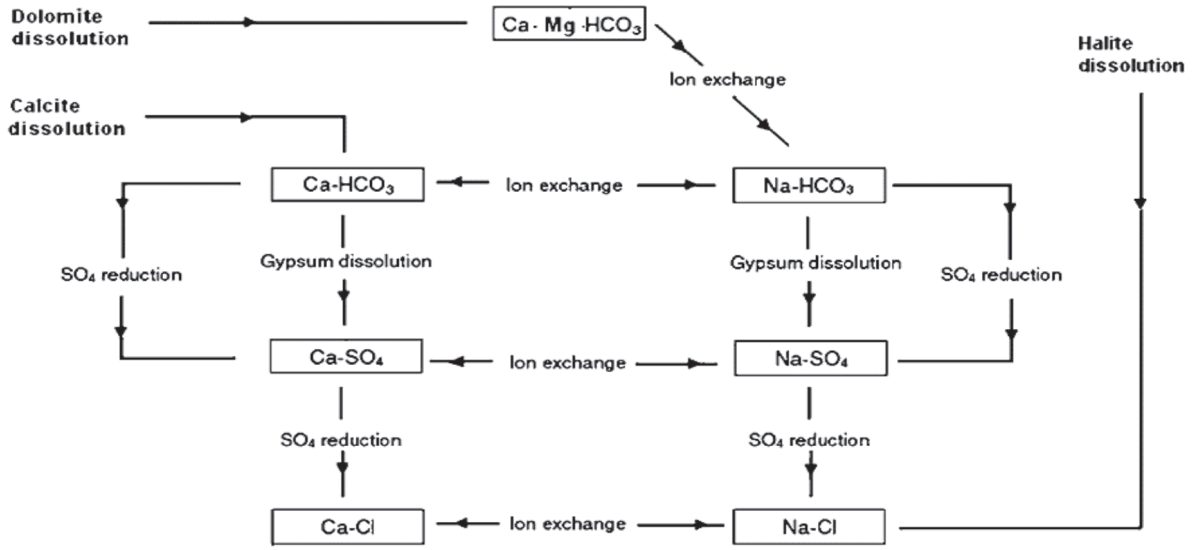

Fig. 5. The effect of various rock water interactions on groundwater types (*Source:* Elango & Kannan, 2007)

is the dissolution of fluorite mineral, while NO_3^- comes from anthropogenic sources (Rezaei *et al.,* 2017). The effect of various rock-water interactions on groundwater types is shown in Fig. 5.

Dissolution and precipitation are other important processes as mentioned in Fig. 5. These are terms used to describe the mass transfer that occurs between rock types and groundwater. When groundwater approaches equilibrium with rocks, then dis-solution begins. This procedure goes on until the mineral components in the groundwater are saturated. The minerals may continue to dissolve at equilibrium therefore, surplus mineral components will mix in the solution to produce precipitates of that particular mineral, which is known as precipitation. Saturation indices (SI) can be used to determine the chemical equilibrium of groundwater for a particular mineral. The SI values less than zero indicate that more mineral is getting dissolved into the solution, depicting the process of dissolution.

$$SI = \frac{\log_{10} IAP}{Ks} \qquad \text{(eq.6)}$$

where IAP is the ionic activity product and K_s is the solubility product of the mineral

Hydrolysis is also an important process that occurs during the rock-water interactions. It is a chemical reaction in which the addition of a molecule of water splits the substance into two halves. However, it is different from the hydration process in which a water molecule is added but no cleavage takes place. Rock and soil components disintegrate into various compounds as a result of hydrolysis (Elango & Kannan 2007). Oxidation-reduction is another important process. Oxidation is caused by the loss of electrons, while reduction is caused by the gain of them. Dissolved oxygen, oxo-anions like NO_3^- and SO_4^{2-}, and water are the most prominent oxidizing agents in groundwater. Organic compounds including inorganic sulphides like pyrite and iron silicates act as reducing agents. Sulfate and iron are typical components in Soil* and groundwater that engage in oxidation and reduction processes. Iron in groundwater is found in two oxidation states: soluble ferrous iron (Fe^{2+}) and oxidized insoluble ferric iron (Fe^{3+}) (Elango & Kannan 2007). The sulfate ions in water may also be lowered as a result of the reduction process. Sulfate reduction is recognized by the SO_4^{2-}/Cl^- ratio. A low SO_4^{2-}/Cl^- ratio indicates that sulfate is being reduced, possibly due to sulfate reduction (Datta & Tyagi, 1996).

The rock-water interactions are identified by the following ionic ratios:

1. Mg^{2+} v/s Ca^{2+}
2. Na^+ v/s Cl^-
3. (Ca^{2+} + Mg^{2+}) v/s (SO_4^{2-} + HCO_3^-)
4. Total Cations v/s (Ca^{2+} + Mg^{2+})

1. Mg^{2+} v/s Ca^{2+}

This plot identifies the most prevailing process among calcite, dolomite, and silicate dissolution. The concentration of Mg^{2+} ions is plotted on the y-

axis while Ca^{2+} is on the x-axis. On the scatter diagram, if the sample plots lie along the aquiline, then this indicates the dissolution of the dolomite mineral as it provides equal concentrations of Ca^{2+} and Mg^{2+} ions. If $1< Ca^{2+}/Mg^{2+} <2$ i.e., higher Ca^{2+} concentration that indicates more calcite weathering. While if the ratio is more than 2 i.e., $Ca^{2+}/Mg^{2+} >2$ then silicate weathering is the prominent source of higher Ca^{2+} ions, especially from plagioclase weathering. Fig. 6a depicts the scatter plot of Mg^{2+} v/s Ca^{2+} of Coimbatore, Tamil Nadu, indicating that maximum samples lie along the 1:1 slope line depicting the dominance of dolomite weathering (Kumar & James, 2016).

2. Na^+ v/s Cl^-

The Na^+ concentration is plotted on the y-axis and the Cl^- concentration on the x-axis. On the scatter diagram if the samples lie along the 1:1 slope line then it depicts the dissolution of halite which gives equal concentrations of Na^+ and Cl^-. However, if the Na^+/Cl^- ratio is less than one i.e., the plots lie below the 1:1 line indicating lower Na^+ concentration, then it depicts the influence of reverse ion exchange mechanism which decreases the Na^+ concentration in groundwater. On the other hand, if the Na^+ concentration comes out to be more than that of Cl^- i.e., $Na^+/Cl^- > 1$, then it estimates the existence of silicate weathering and ion exchange process that increases Na^+ concentration. The Na^+ v/s Cl^- scatter diagram of the north-western region of China is shown in (Fig. 6b). Clearly, the plot shows $Na^+/Cl^- > 1$, thus depicting the domination of silicate weathering and ion exchange process in the region (Feng *et al.,* 2020).

3. $(Ca^{2+}+ Mg^{2+})$ v/s $(SO_4^{2-} + HCO_3^-)$

In this ionic ratio, $(Ca^{2+}+ Mg^{2+})$ is plotted on the y-axis and $(SO_4^{2-} + HCO_3^-)$ on the x-axis. This scatter diagram depicts the dissolution of carbonates and silicates. The dissolution of carbonate minerals like calcite, and dolomite will increase the concentration of Ca^{2+} and Mg^{2+} ions in groundwater (Meybeck 1987)., An increase in the concentration of SO_4^{2-} and HCO_3^- indicates the existence of gypsum and silicate weathering respectively. Therefore, if the points lie above the 1:1 slope line then this will indicate carbonate weathering and vice-versa will point towards silicate and gypsum dissolution (Kumar *et al.,* 2009). However, if the sample points lie along the 1:1 line then both carbonate and silicate weathering are dominant in affecting the groundwater chemistry. In the $(Ca^{2+}+ Mg^{2+})$ v/s $(SO_4^{2-} + HCO_3^-)$ scatter diagram of Sindhudurg district of Maharashtra (Fig. 6c), the majority of groundwater samples lie along the 1:1 line, thus indicating the existence of both carbonate and silicate weathering prevailing in the region (Naidu *et al.,* 2021).

4. Total Cations v/s $(Ca^{2+} + Mg^{2+})$

The probability of silicate weathering as a prominent process is determined by plotting total cations on the y-axis and $(Ca^{2+} + Mg^{2+})$ on the x-axis. Major cations that contribute to total cations are Na^+, K^+, $Mg^{2+,}$ and Ca^{2+}. If the sample points lie above the equiline (1:1) i.e., total cations are more than $(Ca^{2+} + Mg^{2+})$, then this indirectly indicates the presence of more Na^+ ions in groundwater. The higher Na^+ ions are majorly due to silicate weathering or may be due to the ion exchange process. On the other hand, if plots lie below the 1:1 line, depicting a higher concentration of $(Ca^{2+} + Mg^{2+})$, then this may be due to higher carbonate dissolution or reverse ion exchange process. The total cations v/s $(Ca^{2+} + Mg^{2+})$ scatter diagram of the Coimbatore district of Tamil Nadu is shown in Fig. 6d, in which most of the samples are plotted above the aquiline, indicating the supremacy of silicate weathering in the region (Kumar & James 2016).

Weathering Pathways

The type of mineral getting weathered is discussed above but the kind of weathering agent responsible for it needs to be identified. There are two major natural weathering processes, one is the attack of carbonic acid and the other is that of sulphuric acid on various minerals (Meybeck, 1987). For the weathering of carbonates, a source of proton is necessarily required. This proton can be provided by either sulphuric acid or carbonic acid (Das & Kaur, 2001). The weathering reactions of calcite and dolomite minerals are shown below:

Sulphuric acid as a weathering agent

If sulphuric acid acts as the weathering agent, then it's one molecule reacts with one molecule of calcium carbonate (Calcite) resulting in one molecule of calcium and one molecule of sulphate, equation 7. While reacting with dolomite there is a production of one molecule of calcium and two molecules of sulphate, equation 8.

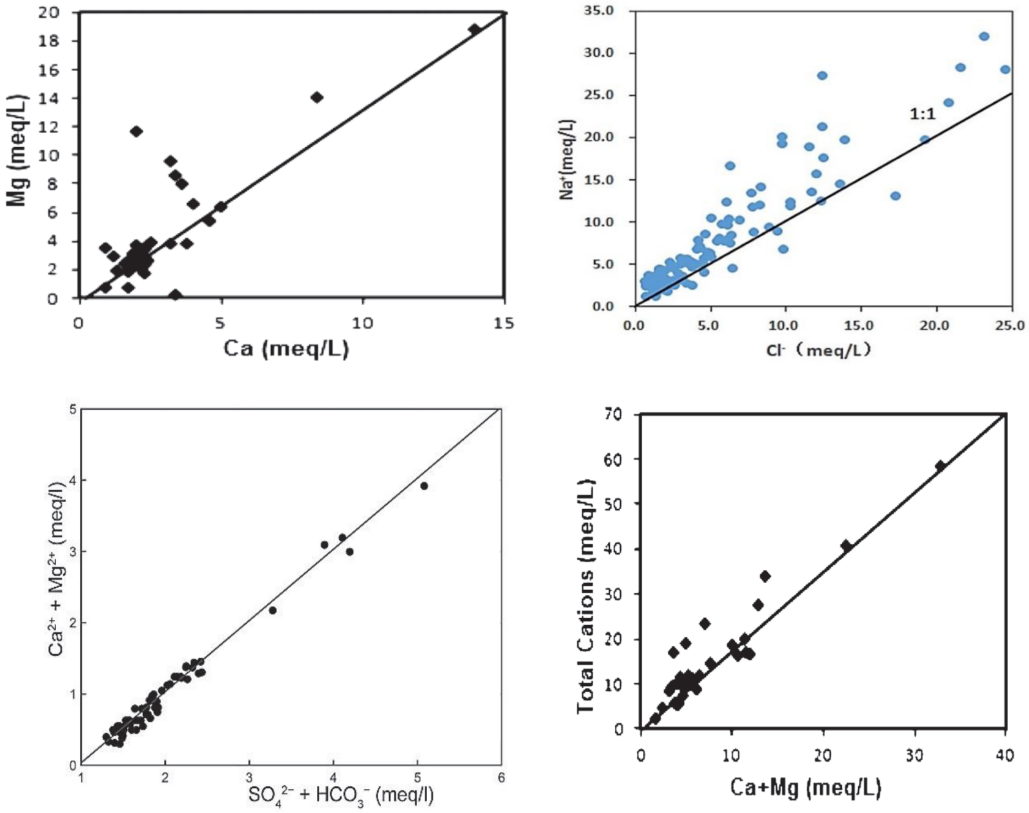

Fig. 6. Scatter plots of various cations and anions. a) Mg^{2+} v/s Ca^{2+} plot of Coimbatore district of Tamil Nadu (*Source:* Kumar & James, 2016), b) Na+ v/s Cl- a plot of north-western China (source: Feng et al. 2020), c) (Ca^{2+}+ Mg^{2+}) v/s (SO_4^{2-} + HCO_3^-) plot of Sindhudurg, Maharashtra (*Source:* Naidu *et al.*, 2021), and d) Total cations v/s (Ca^{2+} + Mg^{2+}) scatter diagram of Coimbatore, Tamil Nadu (*Source:* Kumar & James, 2016)

$$CaCO_3 + H_2SO_4 \text{ ———— } Ca^{2+} + SO_4^{2-} + H_2CO_3 \quad \text{(eq.7)}$$

$$CaMg(CO_3)_2 + 2H_2SO_4 \text{ ———— } Ca^{2+} + Mg^{2+} + 2SO_4^{2-} + 2H_2CO_3 \quad \text{(eq.8)}$$

Carbonic acid as a weathering agent

If carbonic acid is the weathering agent, then it's one molecule reacts with one molecule of calcium carbonate resulting in one molecule of calcium and two molecules of bicarbonate (eq. 9). While reacting with dolomite there is a production of one molecule of calcium and four molecules of bicarbonates (eq. 10).

$$CaCO_3 + H_2CO_3 \text{ ———— } Ca^{2+} + 2HCO_3^- \quad \text{(eq.9)}$$

$$CaMg(CO_3)_2 + 2H_2CO_3 \text{ ———— } Ca^{2+} + Mg^{2+} + 4HCO_3^- \quad \text{(eq.10)}$$

From the above reactions, it can be confirmed that the corresponding ratio of Ca: HCO_3 in the water coming from calcite weathering is 1:2, whereas it is 1:4 in the waters from dolomite weathering. However, the Ca: SO_4 ratio would be 1:1 for calcite and 1:2 for dolomite if sulphuric acid is the weathering agent. The Ca^{2+} vs SO_4^{2-} plot of Lar, Iran (Fig. 7), depicts that most of the plots during the wet

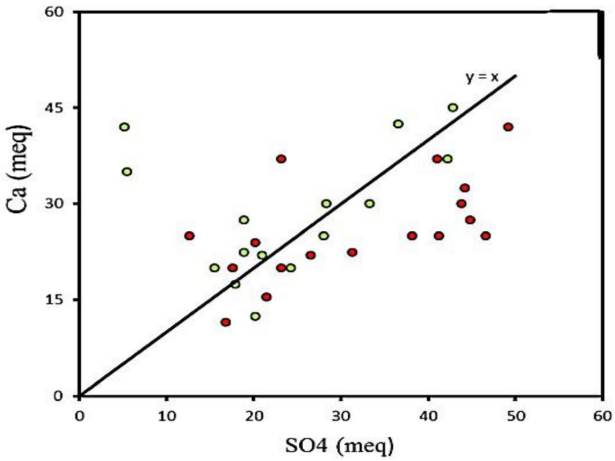

Fig. 7. Ca^{2+} vs SO_4^{2-} plot of Lar, Iran. {Green dots (wet season) and red dots (dry season)} (*Source:* Rezaei *et al.*, 2017)

season (green dots) lie along the 1:1 line indicating the existence of calcite weathering during the season. However, the plots of the dry season (red dots) lie below the 1:1 line, showing a lower concentration of Ca^{2+} as compared to that of SO_4^{2-}, which may be due to calcite weathering or ion exchange process (Rezaei *et al.,* 2017).

However, the deterioration of silicates is completely inconsistent, which generates a variety of solid as well as dissolved species. As a result, silicate weathering products are sometimes difficult to identify. The general reaction for weathering of silicate rocks using carbonic acid is shown below:

(Na, K, Mg, Ca) silicate + H_2CO_3 ——————— H_4SiO_4 + HCO_3 + Na + K+ Mg+ Ca+ solid products

From the above discussion, it can be said that the proton source, parent rock composition, and solid products of chemical weathering all can influence the number of cations and anions discharged into the solution.

Hydrogeochemical facies for the classification of groundwater

Groundwater can be classified based on the concentration of ions present in them into various types called hydrogeochemical facies. Facies are the results of chemical reactions that occur between aquifer minerals and groundwater. These represent the average concentration of major ions in decreasing order (Valencia & Vargas, 2018). Several diagrams are there to plot the hydrogeochemical processes such Piper and Chadha diagram.

1. Piper diagram

The cations and anions present in groundwater are always in chemical equilibrium. The most abundant cations are "alkaline earth" Ca^{2+}, $Mg^{2+,}$ and "alkali" Na^+, while the most abundant anions are "strong acid" Cl^-, $SO_4^{2-,}$ and weak acid HCO_3^- ion (Piper, 1944). A trilinear diagram was proposed that depicts the various water types based on the concentration of ions. It has two triangles that unite to form a diamond (Fig. 8a). The bottom left triangle is the triangle of cations having a basal axis as the axis of Ca^{2+}, while the left and right are the axes of Mg^{2+} and (Na^+ + K^+) respectively. The bottom right triangle is the triangle of anions having the basal axis as the axis of Cl^-, while the left and right are the axes of (CO_3^{2-} + HCO_3^-) and SO_4^{2-} respectively. The union of these two triangles forms a diamond which is broadly classified into four hydrogeochemical facies as described below and shown in Fig 8b.

a. Weak acids exceed strong acids
b. Strong acids exceed weak acids

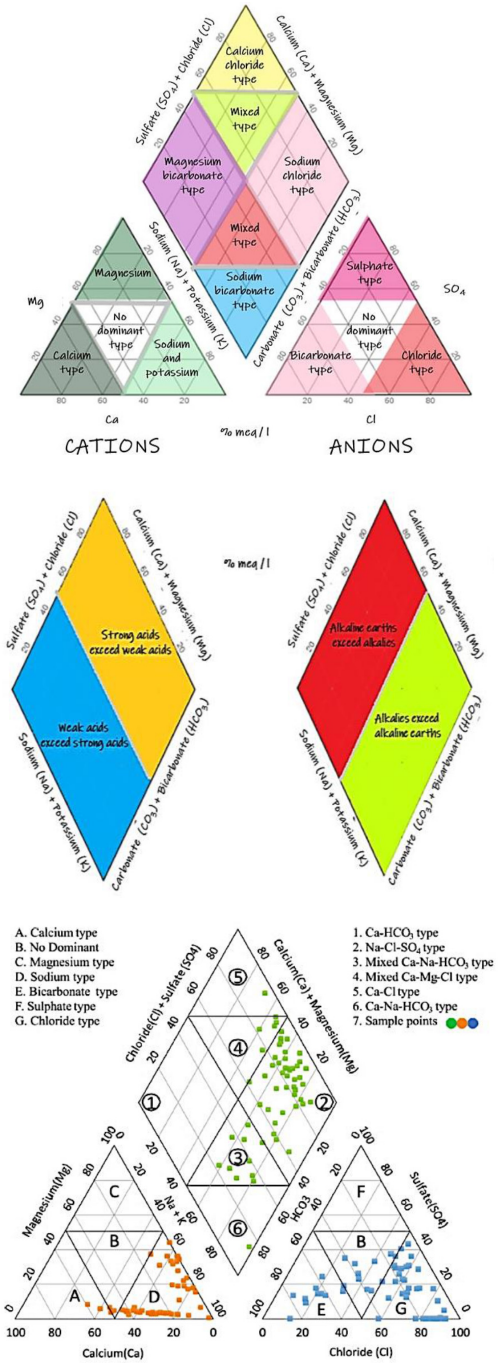

Fig. 8. a) Graphical representation of Piper diagram showing the hydrogeochemical facies (*Source:* Piper, 1944), b) Diamond showing the Hydrogeochemical facies (*Source:* Piper, 1944), and c) Piper diagram of Wanaparthy watershed, Telangana (*Source:* Vaiphei *et al.*, 2020).

c. Alkaline earths exceed alkalies

d. Alkalies exceed alkaline earths

The piper diagram of Wanaparthy watershed, Telangana (Fig. 8c) depicts Na-Cl being the most dominant groundwater type followed by Ca-Na-HCO_3 type. The concentration of anions is in the order $Cl^- > HCO_3^-$, while Na^+ is the most dominant cation subsequently Ca^{2+} (Vaiphei *et al.,* 2020).

2. Chadha diagram

For the identification of hydrogeochemical processes and the categorization of natural waters, a recent hydrochemical diagram is proposed. Trilinear diagrams have several drawbacks which are supposed to be overcome by the Chadha diagram. Piper diagram does not depict the real concentration of ions. The Piper diagram lacks some logic because the distribution of ions inside the main field is not systematic in terms of hydrochemical processes. The strategy of plotting points in the Piper diagram is not very practical when plotting a large amount of data. The two equilateral triangles are absent from the proposed diagram compared to the Piper's, and the main study field is shaped differently. On the Y-axis of the proposed diagram, the difference in milliequivalent % between weak acidic anions and strong acidic anions is plotted, while the difference in milliequivalent percentage between alkaline earth and alkali metals is plotted on the X-axis (Fig. 9a). It is rectangular which is further divided into eight subfields that define the primary character of water (Chadha, 1999). The eight subfields marked from 1 to 8 in Fig. 9a are described below:

a. 1st: Alkaline earths have higher concentration than alkali metals

b. 2nd: The concentration of alkali metals is more than alkaline earth

c. 3rd: The concentration of weak acidic anions exceeds the strong acidic anions

d. 4th: Strong acidic anions have higher concentration than weak acidic anions

e. 5th: Both alkaline earth and weak acidic anions have concentrations higher than alkali metals and strong acidic anions. This type of water has temporary hardness and is of Ca^{2+}-Mg^{2+}-HCO_3^- type

f. 6th: Alkaline earths have higher concentration than alkali metals, while the concentration of strong acidic anions exceeds the weak acidic anions. This type of water has permanent hardness and is of Ca^{2+}-Mg^{2+}-Cl^- type. Usually, the reverse ion exchange process is prominent in the area where this water exists

g. 7th: Alkali metals have higher concentrations than alkaline earth, while the concentration of strong acidic anions is higher than weak acidic anions. Water is of Na^+-Cl^-/SO_4^{2-} type, which can create the problem of salinity

h. 8th: Alkali metals have higher concentrations than alkaline earths, while the concentration of weak acidic anions is more than strong acidic anions. The type of water is sodic in nature and is of Na^+-HCO_3^-.

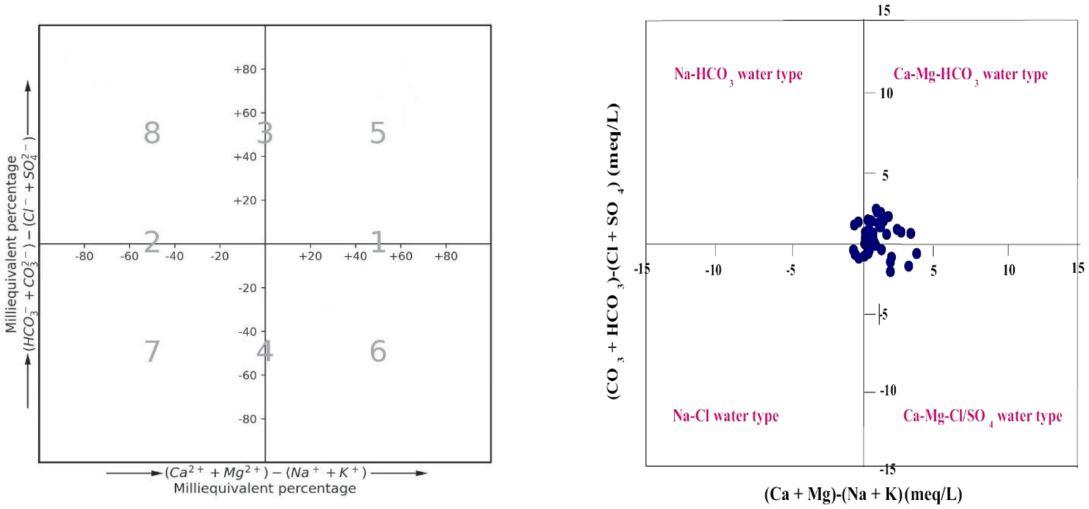

Fig. 9. a) Graphical representation of Chadha diagram (*Source:* wqchartpy, n.d.), and b) Chadha diagram of Korba, Chhattisgarh (*Source:* Singha & Pasupuleti, 2020)

The Chadha diagram of Korba district, Chhattisgarh depicts that Ca-Mg-HCO_3 is the most dominant groundwater type as most of the samples fall in this subfield followed by Ca-Mg-Cl/SO_4^{2-} type (Fig 9b). So, the water in the area has temporary hardness. In general, the concentration of alkaline earths is more than that of alkalis, while weak acidic anions are dominant over strong acidic anions (Singha & Pasupuleti, 2020).

Anthropogenic Sources

Natural processes along with human activities can have an impact on groundwater quality and its hydrochemistry. Natural processes, non-point runoff from agricultural and urban areas, waste dumping techniques, spills and other accidental/ purposeful discharges are all examples of how the chemical composition of groundwater can be altered. When human activities such as urban, industrial, and agricultural operations are the major source and cause of groundwater quality deterioration, the contamination is termed as anthropogenic in nature.

Agricultural activities: Agricultural activities such as extreme use of synthetic pesticides, herbicides, fertilizers, and animal feces, could cause of anthropogenic pollution. Groundwater pollution occurs when industrial wastewater is injected into the hydrological cycle before even being appropriately managed. The dumping of wastes associated with material storage and transportation in production, processing, and construction is another form of groundwater contamination. (CGWB, 2015).

The presence of NO_3^- in groundwater has been identified as a growing concern for groundwater safety and human health. The widespread use of nitrogenous fertilizers is regarded as the key cause of nitrate (NO_3^-) pollution in soil and groundwater. The solubility of NO_3^- in water is high, but soil retention is low. If NO_3^- is not used by plants or is denitrified into N_2 and N_2O, then it is easily leached into the subsoil layer and eventually into groundwater. Drinking water with high NO_3^- levels can cause a variety of health problems in humans (Ahada and Suthar, 2018). Singh (2008) studied the geometric mean nitrate-N content in groundwater samples collected from 21 to 38 m deep tube wells located in cultivated fields in different blocks of Punjab was 3.62 mg/l. About, 78 and 72 percent of the samples were classified under less than 5 and 5–10 mg/l of NO_3–N respectively (Table 2). In regions under rice, maize, and orchards, higher nitrate N concentrations in groundwater were found. In contrast to the cultivated region, the mean NO_3–N concentration in 367 water samples collected from 9 to 18 m deep hand pumps in village habitations was

Table 2. Levels of nitrate in water samples taken from tube wells within cultivated areas, hand pumps in village habitations, and beneath feedlots in rural areas in the Punjab.

Type of well	Number of samples	NO_3^--N (mg/l)		Percent samples having		
		Mean	Range	< 5mg/l	5-10 mg/l	>10 mg/l
Hand pump	367	5.72 + 2.09	1.00 - 11.28	32	66	2
Tube well	236	3.62 + 1.52	1.00 – 6.72	78	72	0
Feedlots	45	4.73 + 2.24	1.24 - 10.44	47	51	2

Source: Singh (2008)

Table 3. Elemental study of household water samples from Ludhiana and Patiala: mean, range, and MPLI

Element (mg/l)	Wallipur (LUDHIANA)		MPLI	Arnetu (PATIALA)		MPLI	Permissible limits (BIS standards) (mg/l)
	Mean	Range		Mean	Range		
Cr	27.99	14.6- 42.9	559.8	2.80	3.76- 2.06	56	0.05
Mn	88.83	41.7- 167.2	888.3	0.97	0.53- 1.26	9.7	0.1
Ni	0	0-0	0	0.53	0- 3.25	26.5	0.02
Cu	25.07	0- 47.6	16.71	15.18	4.76- 23.4	10.12	0.05- 1.5
Zn	18.7	13.4- 66.6	1.24	3.035	1.95- 4.25	0.202	5- 15
As	0.07	0- 0.3	1.4	0	0-0	0	0.05
Pb	2.69	1.6- 3.3	269	7.039	6.3- 7.96	703.9	0.01
Hg	0.04	0- 0.4	40	0	0-0	0	0.001

Source: Kaur *et al*. (2014)

5.72 mg/l, with 66 and 2% of samples containing 5–10 and >10 mg/l of NO_3–N, respectively. The mean NO_3–N concentration was found to be 4.73±2.24 mg/l in water samples obtained from hand pumps close to animal feedlots or dairy farms, which represent a concentrated supply of animal wastes on the edges of settlements.

Industrial activity

Industries can highly influence the chemical composition of groundwater. Industrial areas have groundwater contamination significant to the type of industry and are far different from that of agriculture areas like the paint industry can add heavy metals like Pb, Cr, and Al, while tannery and textile industries can add Cr, several phenolic substances, etc. Ludhiana the industrial hub of Punjab, India is contributing more metal pollution load (Mn, As, Hg, Cu, Cr, and Zn) into Buddha Nullah, a tributary of the river Sutlej compared to the Patiala district of Punjab (Table 3). Based on this data, it can be said that the groundwater near Buddha Nullah is more polluted than that in the Patiala district, due to a higher heavy metal concentration (Kaur *et al.,* 2014). Diesel fuel used widely in farmlands, abandoned batteries, and paint are all possible sources of lead in groundwater. Some insecticides, such as lead arsenate, contain lead as well. Industrial effluents, pesticides, atmospheric deposition, and herbicides all contribute to arsenic contamination of groundwater.

Mining activities

The mining industry has grown to be a significant contributor to global economic growth. Several minerals, such as iron ore, bauxite, and sand ore are widely used as energy and material sources. However, this sector may have negative consequences for the globe, particularly in terms of the environment. Excessive solid waste and waste waters have remained untreated as a result of over-exploitation of these minerals, exposing biodiversity to harmful pollutants. These harmful emissions, which contain heavy metals as well as other trace components, can percolate and penetrate the soil spontaneously, thus polluting the water (Schwab *et al.,* 2007). Iron ore mining site has a significant impact on heavy metal accumulation in the surface water. Bukit Ibam and Kuala Lipis are two mining sites for iron ore in Malaysia (Madzin *et al.,* 2017). Four sampling locations were selected in both Kuala Lipis and Bulkit ibam. The heavy metal concentrations found after analyzing water samples taken from these sites are shown in Table 4. The concentrations of manganese are found to be higher at almost all sites, while that of iron is higher at two sites of Kuala Lipis and aluminum at one site of Bukit Ibam. Mn is a frequent metalloid found in iron ore mining, and because the water pH is alkaline, it may not dissolve easily and thus remain in water. Hence, Mn tends to remain in solution and can be transferred downstream and ultimately into household waters. Al is also found in iron ore and it is extremely difficult to eliminate. Therefore, responsible for various aquatic pollutions.

Table 4. Concentration of heavy metals in surface water at different locations of two mining sites in Malaysia

Location	Cu (mg/l)	Fe (mg/l)	Mn (mg/l)	Zn (mg/l)	Al (mg/l)
		Kuala Lipis			
S1	0.003	1.299	0.297	0.008	0.130
S2	0.002	0.377	0.770	0.005	0.084
S3	0.005	0.286	0.106	0.005	0.079
S4	0.006	0.111	0.010	0.003	0.160
		Bukit Ibam			
S5	0.025	0.104	1.027	0.642	0.345
S6	0.002	0.069	0.068	0.044	0.190
S7	0.011	0.039	0.287	0.017	0.089
S8	0.066	0.039	0.104	0.008	0.054

Source: Madzin *et al*. (2017)

CONCLUSION

Globally groundwater is an important and reliable source for irrigation, drinking, and various other purposes. Groundwater quality of different regions varies depending upon geogenic and anthropogenic activities. Hydrogeochemical processes like rock-water interactions, evaporation, etc. can significantly affect the groundwater quality. Seasonal and geographical fluctuations in groundwater chemistry are largely due to these factors. Various methods and techniques are available for the identification of these hydro-geochemical processes such as Gibbs diagram, rock-water interaction and precipitation. The ion exchange process is another important phenomenon occurring in soil. Chloro-alkaline index and some scatter diagrams are there to identify whether ion exchange or reverse ion exchange is taking place. But no single method can accurately predict a particular process, we require several indicators to do so. Anthropogenic activities like excessive use of

fertilizers, disposal of untreated waste from industries, mining activities, etc., can influence the groundwater quality by increasing NO_3^- and heavy metal concentration in water. Piper and Chadha diagrams can be used for the categorization of groundwater into different hydrogeochemical facies. This integrated approach can be used to establish a groundwater quality prediction model that will aid more precise groundwater monitoring and formulation of different management policies. Groundwater quality must be assessed regularly, and different hydrogeochemical processes must be identified so that suitable management plans can be designed to prevent its deterioration.

STATEMENTS AND DECLARATIONS

Funding

This research did not receive any specific grant from funding agencies in the public, commercial, or not-for-profit sectors.

Competing interests

The authors have no relevant financial or non-financial interests to disclose

Data availability

Data available on request from the authors

Permission to reproduce material from other sources

Copyright permission for reproduced material is taken

REFERENCES

Adimalla N (2020) Controlling factors and mechanism of groundwater quality variation in the semiarid region of South India: an approach of water quality index (WQI) and health risk assessment (HRA). Environ Geochem Health 42(6):1725–1752. https://doi.org/10.1007/s10653-019-00374-8

Ahada CPS & Suthar S (2018) Groundwater nitrate contamination and associated human health risk assessment in southern districts of Punjab, India. Environ Sci Pollut Res 25(25):25336–25347. https://doi.org/ 10.1007/s11356-018-2581-2

Central Groundwater Board (2015) *Bhujal Manthan – a national dialogue on clean and sustainable groundwater*. Retrieved from http://cgwb.gov.in/Bhujal-manthan/Anthropogenic%20pollution_revised.pdf

Chadha DK (1999) A proposed new diagram for geochemical classification of natural waters and interpretation of chemical data. Hydrogeol J 7(5):431-439. https://doi.org/ 10.1007/s100400050216

Cloutier V, Lefebvre R, Savard MM & Therrien R (2010) Desalination of a sedimentary rock aquifer system invaded by Pleistocene Champlain Sea water and processes controlling groundwater geochemistry. Environ Earth Sci 59(5):977–994. https://doi.org/10.1007/s12665-009-0091-8

Das BK & Kaur P (2001) Major ion chemistry of Renuka Lake and weathering processes, Sirmaur District

Himachal Pradesh, India. Environ Geol 40(7) 908–917. https://doi.org/ 10.1007/s002540100268

Datta PS & Tyagi SK (1996) Major ion chemistry of groundwater in Delhi area: Chemical weathering processes and groundwater flow regime. J Geol Soc India 47:179-188. Retrieved from https://www.researchgate.net/publication/260719502

Elango L & Kannan R (2007) Chapter 11 Rock-water interaction and its control on the chemical composition of groundwater. Dev Environ Sci Vol. 5 pp. 229–243. https://doi.org/10.1016/S1474-8177(07)05011-5Feng J, Sun

H, He M, Gao Z, Liu J, Wu X & An Y (2020) Quality assessments of shallow groundwaters for drinking and irrigation purposes: Insights from a case study (Jinta Basin, Heihe drainage area, northwest China). Water (Switzerland) 12(10): 2704-2720. https://doi.org/ 10.3390/w12102704

Gibbs RJ (1970) Mechanisms Controlling World Water Chemistry. Science 170(3962): 1088-1090. https://doi.org/10.1126/science.170.3962.1088

Gabriella A, Osae S, Akiti TT, Adomako D, Ganyaglo, Samuel Y, Bam, Edward P K & Hadis A (2010) Hydrogeochemical and groundwater quality studies in the northern part of the dense river basin of Ghana. J Water Resource Prot 2(12):1071–1081. https://doi.org/ 10.4236/jwarp.2010.212126

Global environment facility (2022) Groundwater. Retrieved from https://www.thegef.org/what-we-do/topics/groundwater.

Fisher RS, & Mullican WF (1997) Hydrochemical evolution of sodium-sulfate and sodium-chlorigroundwater beneath the northern Chihuahuan desert, trans-pecos, Texas, USA. Hydrogeol J 5(2): 9-18. https://doi.org/10.17533/udea.redin.n86a02

Jankowski J & Acworth RI (1997) Impact of debris-flow deposits on hydrogeochemical processes and the development of dryland salinity in the Yass River catchment, New South Wales, Australia. Hydrogeol

J 5(4):71-88. https://doi.org/10.1007/s10040 0050119

Kaur T, Bhardwaj R & Arora S (2017) Assessment of groundwater quality for drinking and irrigation purposes using hydrochemical studies in Malwa region, southwestern part of Punjab, India. Appl Water Sci 7(6):3301–3316. https://doi.org/ 10.1007/s13201-016-0476-2

Kaur T, Sharma K & Sinha AK (2014) Extent of heavy/ trace metals/elements contamination of groundwater resources in Ludhiana and Patiala, Punjab. Man India 94(4): 585-596. Retrieved from https://www.researchgate.net/publication/ 265790781

Kolahchi Z & Jalali M (2007) Effect of water quality on the leaching of potassium from sandy soil. J Arid Environ 68(4):624–639. https://doi.org/10.1016/ j.jaridenv.2006.06.010

Kumar M, Kumari K, Singh UK & Ramanathan A (2009) Hydrogeochemical processes in the groundwater environment of Muktsar, Punjab: Conventional graphical and multivariate statistical approach. Environ Geol 57(4):873–884. https://doi.org/ 10.1007/s00254-008-1367-0

Madzin Z, Kusin FM, Mohd Yusof FM & Muhammad SN (2017) Assessment of water quality index and heavy metal contamination in active and abandoned iron ore mining sites in Pahang, Malaysia. MATEC Web Conf 103: 05010. https://doi.org/10.1051/ matecconf/201710305010

Meybeck M (1987) Global chemical weathering of surficial rocks estimated from river dissolved loads. Am J sci 287(5):401-428. https://doi.org/10.2475/ajs.287. 5.401

Nagaraju A, Muralidhar P & Sreedhar Y (2016) Hydrogeochemistry and groundwater quality assessment of rapur area, Andhra Pradesh, south India. J Geosci Environ Prot 4(4):88–99. https:// doi.org/10.4236/gep.2016.44012

Naidu S, Gupta G, Singh R, Tahama K & Erram VC (2021) Hydrogeochemical processes regulating the groundwater quality and its suitability for drinking and irrigation purposes in parts of coastal Sindhudurg district, Maharashtra. J Geol Soc India 97(2):173–185. https://doi.org/10.1007/s12594-021-1649-7

Piper AM (1944) A graphic procedure in the geochemical interpretation of water-analyses. Eos, Transactions American Geophysical Union, 25(6) pp.914–928. https://doi.org/10.1029/tr025i006p00914

Rezaei M, Nikbakht M & Shakeri A (2017) Geochemistry and sources of fluoride and nitrate contamination of groundwater in Lar area, south Iran. Environ Sci Pollut Res 24(18): 15471–15487. https://doi.org/ 10.1007/s11356-017-9108-0

Sajil Kumar PJ & James EJ (2016) Identification of hydrogeochemical processes in the Coimbatore district, Tamil Nadu, India. Hydrol Sci J 61(4):719–731. https://doi.org/ 10.1080/ 02626667.2015.1022551

Schoeller H (1967) Qualitative evaluation of groundwater resources (in methods and techniques of groundwater investigation and development. Water Resource Series, 33: 44-52.

Schwab P, Zhu D & Banks MK (2007) Heavy metal leaching from mine tailings as affected by organic amendments. Bioresour Technol 98(15):2935–2941. https://doi.org/10.1016/j.biortech.2006.10.012

Singh B, Tiwari MK & Abrol YP (2008) *Reactive nitrogen in agriculture, industry and environment in India.* New Delhi: Indian National Science Academy. Retrieved from https://www.researchgate.net/publication/ 279559843

Singha SS & Pasupuleti S (2020) Hydrogeochemical modeling-based approach for evaluation of groundwater suitability for irrigational use in Korba district, Chhattisgarh, Central India. SN Appl Sci 2(9). https://doi.org/10.1007/s42452-020-03357-y

Subramani T, Rajmohan N & Elango L (2010) Groundwater geochemistry and identification of hydrogeochemical processes in a hard rock region, Southern India. Environ Monitor Assess 162(1–4):123–137. https://doi.org/10.1007/s10661-009-0781-4

Valencia JO & Vargas TB (2018) Hydrogeochemical characterization and identification of a system of regional flow. Case study: the aquifer on the Gulf of Urabá, Colombia. Revista Facultad de Ingeniería Universidad de Antioquia 86:9-18. https://doi.org/ 10.17533/udea.redin.n86a02

Vaiphei SP, Kurakalva RM & Sahadevan DK (2020) Water quality index and GIS-based technique for assessment of groundwater quality in Wanaparthy watershed, Telangana, India. Environ Sci Pollut Res 27(36):45041–45062. https://doi.org/ 10.1007/ s11356-020-10345-7

Wqchartpy (n.d.) Retrieved from https://libraries.io/ pypi/wqchartpy.

Yusuf MA, Abiye TA, Ibrahim KO & Abubakar HO (2021) Hydrogeochemical and salinity appraisal of the surficial lens of freshwater aquifer along Lagos coastal belt, South West, Nigeria. Heliyon 7(10): e08231. https://doi.org/10.1016/j.heliyon. 2021.e08231